Tellus SERIES B CHEMICAL AND PHYSICAL METEOROLOGY
PUBLISHED BY THE INTERNATIONAL METEOROLOGICAL INSTITUTE IN STOCKHOLM

Tellus (2011), 63B, 302–308

TELLUS

Importance of mixing ratio for a long-term CO_2 flux measurement with a closed-path system

By TARO NAKAI*, HIROKI IWATA and YOSHINOBU HARAZONO, *International Arctic Research Center, University of Alaska Fairbanks, Fairbanks, AK 99775-7340, USA*

(Manuscript received 21 January 2011; in final form 14 April 2011)

ABSTRACT

The new type closed-path CO_2/H_2O infrared gas analyser enables us to calculate CO_2 fluxes from both the mixing ratio (F_c^{MR}) and mass density of CO_2 (F_c^{WPL}). After the WPL correction was applied, F_c^{MR} and F_c^{WPL} were almost in accord with each other. However, F_c^{WPL} tended to be slightly larger than F_c^{MR}, which resulted in a significant difference in cumulative CO_2 fluxes. We found that this difference was explained by the pressure covariance term, which is normally omitted in the WPL correction. Therefore, ignoring the pressure covariance term in the WPL correction can cause a serious error in estimation of annual net ecosystem exchange. To reduce uncertainties in calculations, we recommend using the mixing ratio for calculation of CO_2 fluxes when using the new type closed-path infrared gas analyser.

1. Introduction

Recently the new type closed-path CO_2/H_2O infrared gas analysers, such as the LI-7200 (LI-COR, Lincoln, Nebraska, USA) (Burba et al., 2010) and the EC155 (Campbell Scientific, Logan, Utah, USA), were released. Since these employ the closed-path system, they enable us to measure fluxes of CO_2 and water vapour with little data loss during precipitation and no surface heating issue (Burba et al., 2008) compared with the open-path gas analysers. Moreover, these analysers are designed to be installed outdoors and have a short intake tube length, thus making flux attenuation losses in the intake tube smaller compared with the ordinary closed-path analysers (Burba et al., 2010). Burba et al. (2010) confirmed that the hourly CO_2 and water vapour fluxes by the LI-7200 were within 2.5% of the standards measured by the LI-7000 closed-path gas analyser (LI-COR) and the LI-7500 open-path gas analyser (LI-COR), respectively.

In addition, since such analysers measure temperature and pressure in the cell simultaneously with concentrations of CO_2 and water vapour, variations in mixing ratios of CO_2 and water vapour are available directly. This enables us to obtain fluxes of CO_2 and water vapour without applying density correction (Webb et al., 1980) (hereafter WPL correction), as suggested by Leuning (2004). The mixing ratio has advantages over mass density in that it is conserved during thermal expansion/compression and through all hydrological processes such as phase change and water vapour diffusion (Kowalski and Serrano-Ortiz, 2007). Thus the use of the mixing ratio has been recommended by Leuning (2004, 2007), Kowalski and Serrano-Ortiz (2007) and Kowalski (2008) to calculate true eddy fluxes. However, Burba et al. (2010) calculated CO_2 flux using the FluxNet methodology described by Aubinet et al. (2000), that is, from the mass density of CO_2 with the WPL correction even for the LI-7200. Therefore, it is still unknown how the CO_2 flux from the mixing ratio of such a closed-path gas analyser performs.

The scope of this study was to analyse the importance of the mixing ratio for long-term evaluation of CO_2 flux by comparing it with CO_2 mass density flux and clarifying what causes the difference between them.

2. Theory

Since the mixing ratio of CO_2 relative to dry air χ_c (mol mol^{-1}) is measured by the LI-7200, CO_2 flux from the mixing ratio F_c^{MR} (mol m^{-2} s^{-1}) is derived by covariance of χ_c and vertical wind speed w (m s^{-1}) as follows:

$$F_c^{MR} = \overline{\varrho_d}\,\overline{w'\chi_c'}, \tag{1}$$

where ϱ_d (mol m^{-3}) is a molar density of dry air calculated by

$$\overline{\varrho_d} = \left(1 - \overline{f_v}\right) \frac{\overline{p_{cell}}}{R\overline{T_{cell}}}, \tag{2}$$

where f_v (mol mol^{-1}) is a mole fraction of water vapour relative to total (wet) air, $R = 8.31$ (J K^{-1} mol^{-1}) is the gas constant and p_{cell} (Pa) and T_{cell} (K) are pressure and air temperature in the closed-path sampling cell of the LI-7200, respectively. An

*Corresponding author.
e-mail: tnakai@iarc.uaf.edu; taro.nakai@gmail.com
DOI: 10.1111/j.1600-0889.2011.00538.x

overbar denotes a time averaging, and a prime denotes the deviation from the mean. According to the LI-7200 manual (Publication No. 984-10564, 22 July 2009), mole fractions of water vapour f_v and CO_2 f_c (mol mol^{-1}) are calculated from a measured molar density of water vapour ϱ_v and CO_2 ϱ_c (mol m^{-3}) as

$$f_v = \frac{\varrho_v R T_{cell}}{p_{cell}}, \quad (3)$$

$$f_c = \frac{\varrho_c R T_{cell}}{p_{cell}}. \quad (4)$$

Thus the mixing ratio of CO_2 χ_c is derived as follows:

$$\chi_c = \frac{f_c}{1 - f_v}, \quad (5)$$

which is equivalent to the eq. (6.23) by Leuning (2004).

Similarly, CO_2 flux from the mass density of CO_2 ρ_c (kg m^{-3}) with the WPL correction F_c^{WPL} (kg m^{-2} s^{-1}) is calculated as follows:

$$F_c^{WPL} = \overline{w'\rho_c'} + F_V + F_T, \quad (6)$$

where F_V and F_T (kg m^{-2} s^{-1}) are the water vapour covariance term and temperature covariance term of the WPL correction, respectively, described as follows:

$$F_V = \frac{m_d}{m_v} \frac{\overline{\rho_c}}{\overline{\rho_d}} \overline{w'\rho_v'}, \quad (7)$$

$$F_T = \overline{\rho_c} \left(1 + \frac{m_d}{m_v} \frac{\overline{\rho_v}}{\overline{\rho_d}}\right) \frac{\overline{w'T_{cell}'}}{\overline{T_{cell}}}, \quad (8)$$

where $m_d = 28.966$ (Gatley et al., 2008) and $m_v = 18.015$ (kg kmol^{-1}) are the molecular mass of dry air and water vapour, and $\rho_d (= m_d \varrho_d)$ and ρ_v (kg m^{-3}) are the mass density of dry air and water vapour, respectively. Note that the original WPL correction (Webb et al., 1980) neglected the pressure covariance term F_P (kg m^{-2} s^{-1}) (e.g. Lee and Massman, 2011),

$$F_P = -\overline{\rho_c} \left(1 + \frac{m_d}{m_v} \frac{\overline{\rho_v}}{\overline{\rho_d}}\right) \frac{\overline{w'p_{cell}'}}{\overline{p_{cell}}}, \quad (9)$$

since the F_P is expected to be small enough compared to F_V and F_T (Leuning, 2004).

Furthermore, to complete the density correction, two additional terms were provided by Fuehrer and Friehe (2002) and Lee and Massman (2011), that is, the CO_2 self-dilution term F_C (kg m^{-2} s^{-1}) and the higher order temperature term F_H (kg m^{-2} s^{-1}), expressed as follows:

$$F_C = \frac{m_d}{m_c} \frac{\overline{\rho_c}}{\overline{\rho_d}} \overline{w'\rho_c'}, \quad (10)$$

$$F_H = -\overline{\rho_c} \left(1 + \frac{m_d}{m_v} \frac{\overline{\rho_v}}{\overline{\rho_d}}\right) \frac{1}{\overline{T_{cell}}} \overline{\left(\frac{w'T_{cell}'^2}{T_{cell}}\right)}, \quad (11)$$

where $m_c = 44.010$ (kg kmol^{-1}) is the molecular mass of CO_2. Theoretically, these CO_2 fluxes from the mixing ratio and mass density are equal, that is,

$$F_c^{MR} = F_c^{WPL} + F_P + F_C + F_H. \quad (12)$$

3. Measurements

The gas analyser LI-7200 and ultrasonic anemometer WindMaster Pro (Gill Instruments, Lymington, UK) were installed in a burned black spruce forest on a hilltop of the Poker Flat Research Range, University of Alaska Fairbanks, where the ongoing year-round flux observation is conducted (Iwata et al., 2011). At this site, understory plants such as shrubs and herbs have recovered after a wildfire that occurred in 2004. Fractional vegetation cover of these plants was about 70–80%, and their plant height was not more than 0.5 m in the measurement area. The data from 6 August to 14 September 2010 were used and were logged by the LI-7550 (interface unit of LI-7200) at 10 Hz. Measurement height was about 2.5 m above the ground. Length and inner diameter of the intake tube of the LI-7200 were 1.0 m and 9.5 mm, respectively, and flow rate was kept at 15 standard L min^{-1}. At the leading edge of the intake tube, a rain guard/bug screen attachment was installed, and thus the inlet of the intake tube faced downwards.

The pressure in the sampling cell of the LI-7200 p_{cell} is measured using two pressure sensors. One is installed inside the enclosure of the LI-7550 and measures the atmospheric pressure in the enclosure. The other is the differential pressure sensor installed on the LI-7200 sensor head, and it measures the differential pressure between the sampling cell and the LI-7550 enclosure. p_{cell} is the sum of these measurements. The differential pressure sensor measures very fast (about 300 Hz), and it responds immediately to the pressure variation in terms of eddy covariance measurements (George Burba, LI-COR, personal communication, 2011). The temperature in the LI-7200 is measured by the fine thermocouples at the air inlet and outlet [T_{in} and T_{out}, respectively (K)]. The temperature in the sampling cell T_{cell} is represented by $T_{cell} = 0.2T_{in} + 0.8T_{out}$ (LI-COR, personal communication).

In consideration of the delay time t_d (s) between the LI-7200 and the WindMaster Pro, a 'dynamic' delay correction was introduced. This correction explains delays due to the wind speed and direction, flow rate, and internal delay of the LI-7200, LI-7550 and WindMaster Pro. Thus t_d can be expressed as follows:

$$t_d = -\frac{l}{\overline{U}} \cos(\gamma - b) + \frac{AL}{Q} + d, \quad (13)$$

where l(m) is the separation between the sonic anemometer and the inlet of the intake tube, $\overline{U}$(m s^{-1}) is the mean wind speed, γ (rad) is wind direction, b (rad) is direction of the inlet, A (m^2) is the section area of the intake tube, L (m) is the intake tube length, Q (m^3 s^{-1}) is flow rate and d (s) is a time constant explained by the internal process delays of the LI-7200, LI-7500 and WindMaster Pro. Here the positive t_d denotes that the

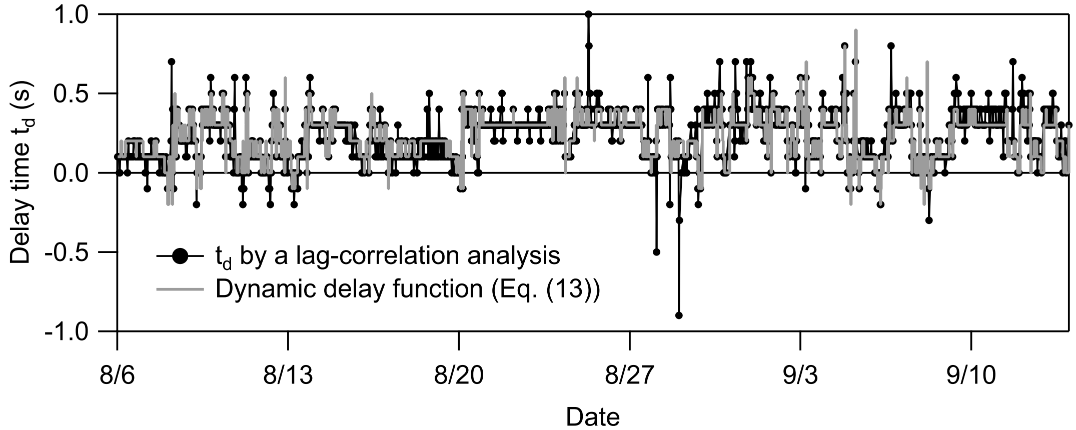

Fig. 1. Comparison between the delay time t_d determined by a lag cross-correlation analysis and that from the dynamic delay function (eq. 13).

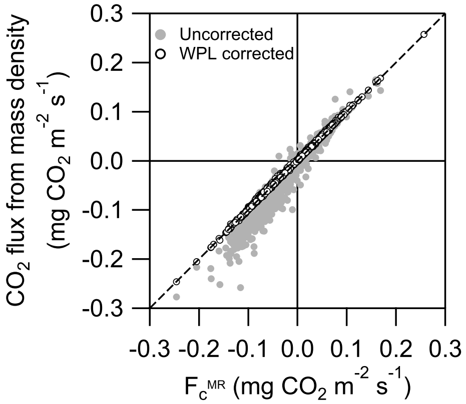

Fig. 2. Comparison between CO_2 flux from the mixing ratio F_c^{MR} and that from mass density before and after WPL correction ($\overline{w'\rho_c'}$ and F_c^{WPL}, respectively).

LI-7200 delays in comparison with the WindMaster Pro. In this study, l, b and d were determined by the least-squares method to fit eq. (13) to the delay time determined by a lag cross-correlation analysis between sonic temperature from the WindMaster Pro and χ_c from the LI-7200. The t_d from eq. (13) well described the delay time determined by a lag cross-correlation analysis (Fig. 1).

Data spikes were removed according to Vickers and Mahrt (1997). The double coordinate rotation was used to make the mean lateral and vertical wind speeds zero (McMillen, 1988). Detrending and corrections of other effects such as frequency response or tube attenuation effects were not applied. Finally, the calculations of CO_2 fluxes were set as the same unit of mg CO_2 m^{-2} s^{-1}.

4. Results

Figure 2 shows the relationship between CO_2 flux from the mixing ratio F_c^{MR} and that from mass density before and after the application of the WPL correction (i.e., $\overline{w'\rho_c'}$ and F_c^{WPL}). After the WPL correction was applied, calculations of F_c^{MR} and F_c^{WPL} were almost in accord with each other. However, F_c^{WPL} tended to be slightly larger than F_c^{MR}, and the difference $F_c^{WPL} - F_c^{MR}$ was positive in most of this period irrespective of day and night (Fig. 3). Though the difference $F_c^{WPL} - F_c^{MR}$ was two orders of magnitude smaller than F_c^{WPL} and F_c^{MR}, it turned out to be a large difference in the cumulative CO_2 fluxes in the whole 5-week period (Fig. 3). The values of the cumulative CO_2 fluxes were $\sum F_c^{MR} = -9.46$ and $\sum F_c^{WPL} = -6.28$ (g m^{-2}).

We found that the difference between F_c^{MR} and F_c^{WPL} was almost the same value with the pressure covariance term F_P, and the difference between F_c^{MR} and $F_c^{WPL} + F_P$ was negligible (Fig. 3). The difference between them in the cumulative CO_2 flux was also small, $\sum(F_c^{WPL} + F_P) = -9.55$ (g m^{-2}), and the difference between $\sum F_c^{MR}$ and $\sum(F_c^{WPL} + F_P)$ was 1.0% of $\sum F_c^{MR}$ (Fig. 4). The magnitudes of both $F_c^{WPL} - F_c^{MR}$ and F_P were dependent on the wind speed, and the effect of the pressure covariance term was greater when wind speed was higher (Fig. 5).

Two additional terms, F_C and F_H, were quite small, and the values of them in cumulative fluxes were $\sum F_C = -1.45 \times 10^{-2}$ and $\sum F_H = -3.21 \times 10^{-4}$ (g m^{-2}) in this period. However, since these values were both negative, the complete mass density flux was cumulated as $\sum(F_c^{WPL} + F_P + F_C + F_H) = -9.57$ (g m^{-2}), and the difference between it and $\sum F_c^{MR}$ was slightly larger than that before F_C and F_H were added.

5. Discussion

The results experimentally confirmed that the measurements of CO_2 flux from the mixing ratio were consistent with those from mass density with the WPL correction including the pressure covariance term. This indicates that ignoring the pressure covariance term in the WPL correction will provide a significant positive shift in the cumulative CO_2 flux estimation, resulting in a serious error in estimation of the annual net ecosystem

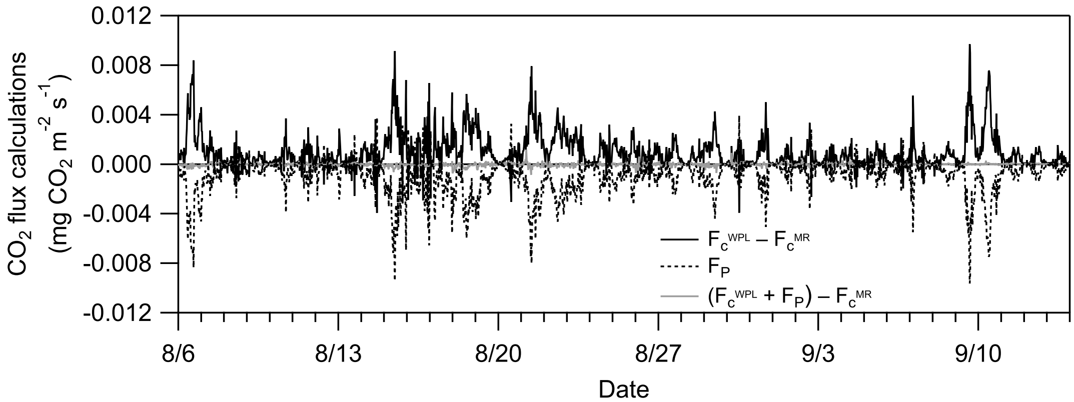

Fig. 3. Variations in the difference between F_c^{WPL} and F_c^{MR}, the pressure covariance term F_P, and the difference of fluxes after F_P was considered.

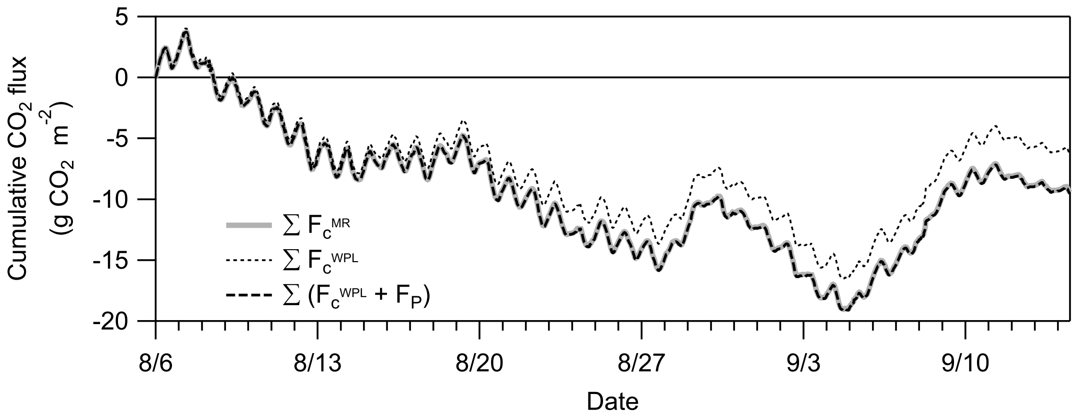

Fig. 4. Comparison of the variations in the cumulative CO_2 fluxes, $\sum F_c^{MR}$, $\sum F_c^{WPL}$ and $\sum(F_c^{WPL} + F_P)$.

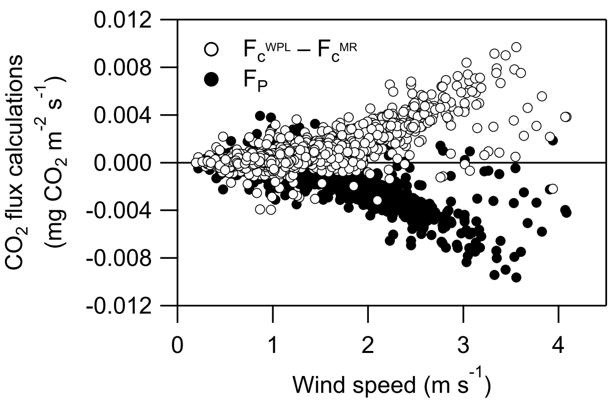

Fig. 5. Relationship between horizontal wind speed and $F_c^{WPL} - F_c^{MR}$, F_P.

exchange (NEE). In addition, according to Fig. 5, the errors in the NEE estimation due to the omission of the pressure covariance term can be large in windy areas. The importance of the pressure covariance term in the long-term CO_2 flux measurement has been pointed out in previous studies (e.g. Massman and Lee, 2002; Massman, 2004; Zhang et al., 2011). Lee and Massman (2011) showed that the cumulative pressure correction accounted for roughly 20% of the annual NEE by using a data set by Zhang et al. (2011), and they pointed out that the pressure covariance term should not be omitted when using the open-path eddy covariance system. However, actual consistency between F_c^{MR} and F_c^{WPL} with the density correction terms had not been checked because F_c^{MR} was unavailable in the previous systems. This study is the first to actually confirm by experiment that the difference between F_c^{MR} and F_c^{WPL} is explained by the pressure covariance term F_P, owing to the development of the new type closed-path gas analyser.

Similarly, this result also shows that the calculation of CO_2 flux from the mixing ratio F_c^{MR} is reliable in that F_c^{MR} accounts for the CO_2 mass density flux including the pressure covariance term of the density correction. The long-term sums of the CO_2 self-dilution term and the higher order temperature term were both negligible, as pointed out by Lee and Massman (2011). F_c^{MR} can be considered as the true surface flux based on the arguments by Bakan (1978) and Webb et al. (1980), and the expressions of CO_2 flux from mass density with density correction terms are much more complex than F_c^{MR}. Therefore, to reduce

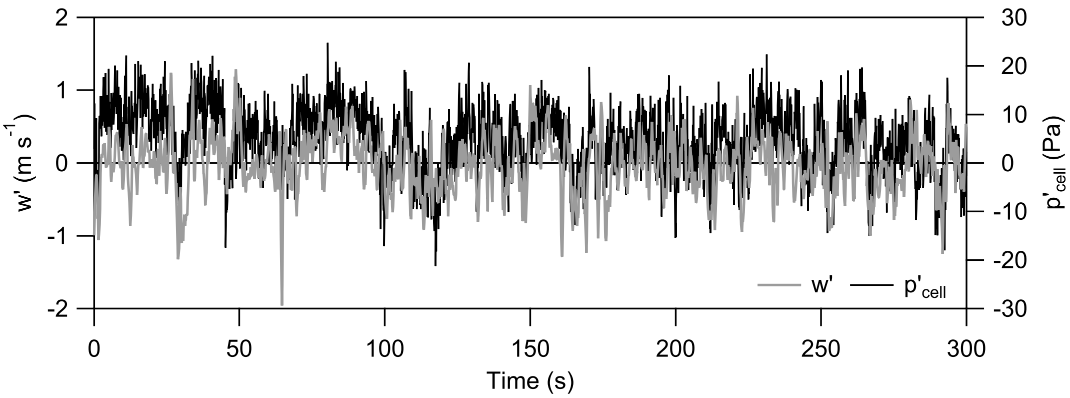

Fig. 6. A typical time series of the variations in the deviations of vertical wind speed in the open air w' and pressure in the closed-path sampling cell of LI-7200p'_{cell}. The data shown here were taken from 11:10 to 11:15 AST, 15 August 2010. Note that these deviations were from the 30 min mean values from 11:00 to 11:30. Delay time of the LI-7200 was corrected by eq. (13).

uncertainties, the mixing ratio is preferable for calculation of CO_2 fluxes when using the new type closed-path infrared gas analysers.

It should be noted that the negative F_{P} in this study (Figs 3 and 5) was due to the positive correlation between vertical wind speed w and pressure in the cell p_{cell} (Fig. 6). This is opposite of the results for the open-path system by Zhang et al. (2011), who measured fluctuations of vertical wind velocity w' and static pressure p' in the open air and showed the negative correlation between them, which resulted in a 'positive' F_{P}. Previous observations on the static pressure fluctuation in the open air support their results, i.e., negative $\overline{w'p'}$ and positive F_{P} (e.g. McBean and Elliott, 1975; Wilczak and Businger, 1984; Massman and Lee, 2002). Note that results of F_{P} by Zhang et al. (2011) and other previous studies were for the open-path flux systems, and the physical mechanisms that underlie the pressure fluctuations are different between open- and closed-path systems. Discrepancy between positive F_{P} in previous studies (open-path) and negative F_{P} in this study (closed-path) is due to the fact that the pressure in this study was measured in the cell with continuous air flow. Nevertheless, since the pressure fluctuations in the p'_{cell} seemed to be systematically related to w' (Fig. 6), and the pressure covariance term F_{P} decreased with the increasing horizontal wind speed (Fig. 5), variation in the p'_{cell} would also be due to the motion of the ambient air. One possible explanation of this phenomenon is that since the inlet of the intake tube faced downwards in this study, horizontal wind was orthogonal to the inlet, and thus the increase of horizontal wind speed resulted in a decrease of pressure inside the intake tube and the sampling cell. Actually, fluctuation in the p_{cell} was mostly explained by the variation in the negative dynamic pressure $-\rho U^2/2$ (Pa) due to the ambient horizontal wind speed U (m s^{-1}) as shown in Fig. 7, where ρ (kg m^{-3}) is the total air density. If this is correct, the pressure covariance term F_{P} can be affected by the presence or absence of the downward-facing rain guard/bug screen attachment. When this attachment is not used, the inlet of the intake tube will open horizontally, and the effect of wind speed on the pressure variation in the cell will depend on the wind direction. These factors should be clarified in future studies.

Figure 8 shows the normalized ensemble average spectrum of the p_{cell} and w-p_{cell} co-spectrum. The slope of the power spectrum was smaller than −3/2, whereas −3/2 slope was observed in the open-air static pressure by Zhang et al. (2011). No clear attenuation of the power spectrum of p_{cell} was found, but

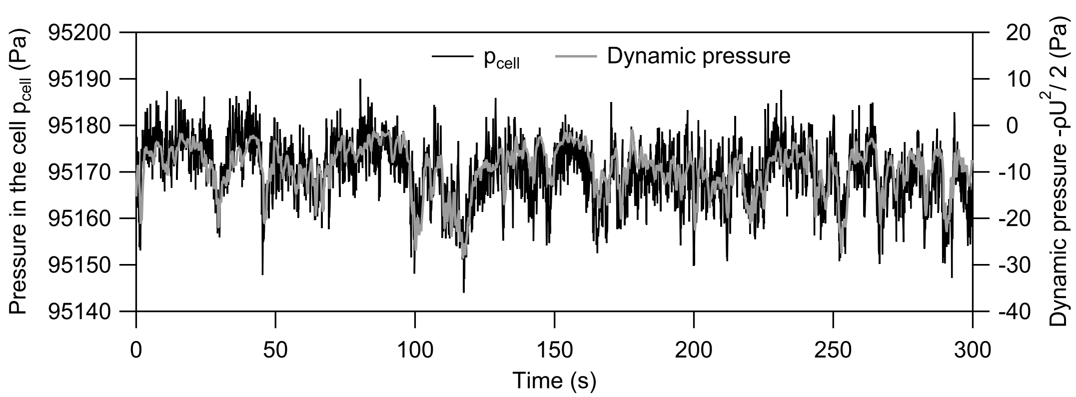

Fig. 7. Variations in the pressure in the sampling cell p_{cell} and the negative dynamic pressure $-\rho U^2/2$. The time period is the same as in Fig. 6.

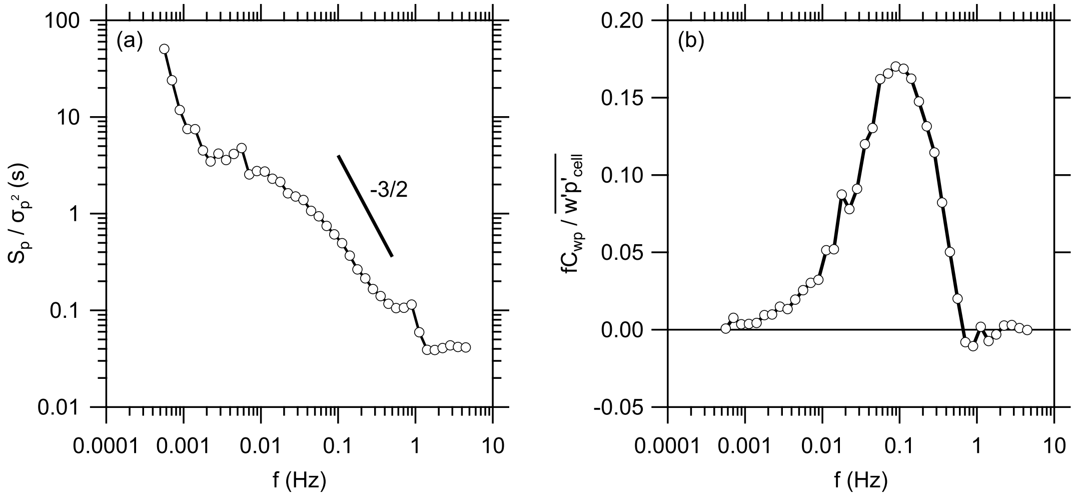

Fig. 8. Ensemble average spectrum of p_{cell}, S_p/σ_p^2 (a), and w-p_{cell} co-spectrum, $fC_{wp}/\overline{w'p'_{cell}}$ (b), where σ_p (Pa) is the standard deviation of p_{cell}. The data under neutral condition [$|z/L| < 0.01$, where $z = 2.5$ (m) is the measurement height and L (m) is Monin-Obukhov length], mean wind speed of $2 < \overline{U} < 5$ (m s^{-1}) and $\overline{w'p'_{cell}} > 0.3$ (Pa m s^{-1}) were used.

$f > 0.5$ Hz seemed to be affected by noise. Nevertheless, most of the covariance $\overline{w'p'_{cell}}$ was accounted for by the frequency range lower than 0.5 Hz.

6. Conclusions

By using the new type closed-path CO_2/H_2O infrared gas analyser, we concluded that the difference between the cumulative CO_2 fluxes from the mixing ratio and mass density was explained by the pressure covariance term of the density correction. It was experimentally confirmed that the measurement of CO_2 flux from the mixing ratio was consistent with that from mass density with the WPL correction including the pressure covariance term. This consistency indicates that the pressure covariance term would also affect the long-term cumulative CO_2 flux measured by an open-path gas analyser, as pointed out by recent studies. Our results confirm the key conclusion by Webb et al. (1980) that the true eddy flux is given by the product of the dry air density and the covariance between the vertical velocity and the mixing ratio of trace gas relative to dry air. To reduce uncertainties, the mixing ratio is recommended in calculating CO_2 fluxes when a new type closed-path infrared gas analyser is employed.

7. Acknowledgments

We thank Shin'ichi Iida, Takanori Shimizu, Yoshikazu Ohtani, Yuichiro Nakai, and Satoru Takanashi of FFPRI and anonymous reviewers for their valuable comments. We also acknowledge Tom Alton of IARC, UAF for the English proofreading of the manuscript. This research was supported in part by the Japan Agency for Marine-Earth Science and Technology (JAMSTEC) and the Japan Aerospace Exploration Agency (JAXA).

References

Aubinet, M., Grelle, A., Ibrom, A., Rannik, U., Moncrieff, J. and coauthors. 2000. Estimates of the annual net carbon and water exchange of forests: the EUROFLUX methodology. *Adv. Ecol. Res.* **30**, 113–175.

Bakan, S. 1978. Note on the eddy covariance method for CO_2 flux measurements. *Boundary-Layer Meteorol.* **14**, 597–600.

Burba, G. G., McDermitt, D., Grelle, A., Anderson, D. and Xu, L. 2008. Addressing the influence of instrument surface heat exchange on the measurements of carbon dioxide flux from open-path gas analyzers. *Global Change Biol.* **14**, 1854–1876.

Burba, G. G., McDermitt, D. K., Anderson, D. J., Furtaw, M. D. and Eckles, R. D. 2010. Novel design of an enclosed CO_2/H_2O gas analyser for eddy covariance flux measurements. *Tellus, Ser. B* **62**, 743–748.

Fuehrer, P. L. and Friehe, C. A. 2002. Flux corrections revisited. *Boundary-Layer Meteorol.* **102**, 415–457.

Gatley, D. P., Herrmann, S. and Kretzschmar, H.-J. 2008. A twenty-first century molar mass for dry air. *HVAC&R Res.* **14**, 655–662.

Iwata, H., Ueyama, M. and Harazono, Y. 2011. A year-round flux observation at an area burned by wildfire in Interior Alaska. *Asiaflux Newsletter* **32**, 13–18.

Kowalski, A. S. 2008. Comment on "The storage term in eddy flux calculations". *Agric. For. Meteorol.* **148**, 691–692.

Kowalski, A. S. and Serrano-Ortiz, P. 2007. On the relationship between the eddy covariance, the turbulent flux, and surface exchange for a trace gas such as CO_2. *Boundary-Layer Meteorol.* **124**, 129–141.

Lee, X. and Massman, W. J. 2011. A perspective on thirty years of the Webb, Pearman and Leuning density corrections. *Boundary-Layer Meteorol.* **139**, 37–59.

Leuning, R. 2004. Measurements of trace gas fluxes in the atmosphere using eddy covariance: WPL corrections revisited. In: *Handbook of Micrometeorology: A Guide for Surface Flux Measurement and Analysis*, (eds. X. Lee, W. Massman and B. Law), Kluwer Academic Publishers, Dordrecht, 119–132.

Leuning, R. 2007. The correct form of the Webb, Pearman and Leuning equation for eddy fluxes of trace gases in steady and non-steady state, horizontally homogeneous flows. *Boundary-Layer Meteorol.* **123**, 263–267.

Massman, W. J. 2004. Concerning the measurements of atmospheric trace gas fluxes with open- and closed-path eddy covariance system: the WPL terms and spectral attenuation. In: *Handbook of Micrometeorology: A Guide for Surface Flux Measurement and Analysis*, (eds. X., Lee, W., Massman and B., Law), Kluwer Academic Publishers, Dordrecht, 133–160.

Massman, W. J. and Lee, X. 2002. Eddy covariance flux corrections and uncertainties in long-term studies of carbon and energy exchanges. *Agric. For. Meteorol.* **113**, 121–144.

McBean, G. A. and Elliott, J. A. 1975. Vertical transports of kinetic-energy by turbulence and pressure in boundary-layer. *J. Atmos. Sci.* **32**, 753–766.

McMillen, R. T. 1988. An eddy correlation technique with extended applicability to non-simple terrain. *Boundary-Layer Meteorol.* **43**, 231–245.

Vickers, D. and Mahrt, L. 1997. Quality control and flux sampling problems for tower and aircraft data. *J. Atmos. Oceanic Tech.* **14**, 512–526.

Webb, E. K., Pearman, G. I. and Leuning, R. 1980. Correction of flux measurements for density effects due to heat and water vapor transfer. *Quart. J. R. Meteorol. Soc.* **106**, 85–106.

Wilczak, J. M. and Businger, J. A. 1984. Large-scale eddies in the unstably stratified atmospheric surface layer, part II: turbulent pressure fluctuations and the budgets of heat flux, stress and turbulent kinetic energy. *J. Atmos. Sci.* **41**, 3551–3567.

Zhang, J., Lee, X., Song, G. and Han, S. 2011. Pressure correction to the long-term measurement of carbon dioxide flux. *Agric. For. Meteorol.* **151**, 70–77.